POLITECNICO
MILANO 1863

SCUOLA DI INGEGNERIA INDUSTRIALE
E DELL'INFORMAZIONE

Executive Summary of the Thesis

A Loosely-Coupled Scheme for Cardiac Electro Fluid Structure Interaction

Laurea Magistrale in Mathematical Engineering - Ingegneria Matematica

Author: Martin Geraint Gabriel

Advisor: Prof. Christian Vergara

Co-advisor: Michele Bucelli

Academic year: 2020-2021

1. Introduction

Fluid Structure Interaction (FSI) problems are present in many fields (e.g. aeroelasticty, industry, living systems) and many kind of algorithms have been designed to solve such problems: from Monolithic schemes to explicit and implicit partitioned ones. The most attractive schemes are for sure the explicit ones; indeed, they are modular, i.e. different already existing solvers can be employed. One of the most challenging fields where FSI is thriving surely is hemodynamics, where the employment of explicit algorithms is tempting but difficult to implement due to their instability caused by the added-mass effect that occurs when comparable densities are at stake. However recent studies have been carried on a particular kind of explicit scheme: the Robin-Neumann scheme [2, 3]. In these just cited works also a theoretical investigation on a simplified problem to find the optimal Robin parameter has been carried out, leading to encouraging results in terms of accuracy and stability, also in realistic cases. We want to apply for the first time such theory to a more complex problem: the cardiac Electro Fluid Structure Interaction (EFSI) Problem arising from the modeling of the ventricular functions. The main difference with respect to other FSI problems is the fact that the myocardium (i.e. the muscular tissue of the ventricle) is not only passive, but it has also an active component driven by electrophysiology, that allows it to actively contract [4]. Finally, the main purpose of this work is to present a new Loosely-Coupled Scheme for the EFSI Problem, aiming to achieve a good level of accuracy, stability and computational cost.

2. Mathematical Models

The human ventricle is schematized in figure 1 and composed by a fluid domain $\hat{\Omega}_f$ covered by the structure domain $\hat{\Omega}_s$, except for the base (divided in $\Gamma_{s,b}$ for the structure base and $\Gamma_{f,b}$ for the fluid base), where two idealized overlapping valve orifices are present: the aortic one (Γ_{AV}) and the mitral one (Γ_{MV}). The fluid and structure domain are separated by the Fluid Structure Interface $\hat{\Sigma}$. We define the two unit vectors normal to the boundaries: $\hat{\boldsymbol{n}}_{\boldsymbol{s}}$ and $\hat{\boldsymbol{n}}_f$ such that $\hat{\boldsymbol{n}} = \hat{\boldsymbol{n}}_f = -\hat{\boldsymbol{n}}_s$ on $\hat{\Sigma}$. Finally, we define the epicardial surface $\Gamma_{s,epi}$, corresponding to the external portion of the structure domain.

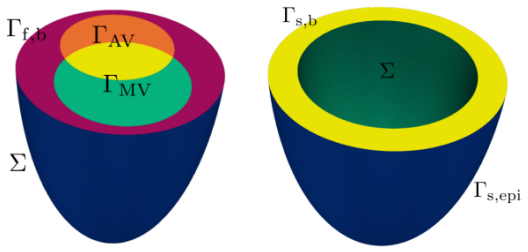

Figure 1: The computational domain [1].

We need to model the different physics defining the following variables and problems. For the sake of simplicity we will make use of an abstract notation to identify the underlying PDEs and ODEs highlighting the different dependencies. The initial and boundary conditions are condensed in the above cited abstract operators, but for the coupling conditions on the Fluid Structure Interface Σ:

- for the Electrophysiologcal Problem we define the transmembrane potential v modeled with the PDE Monodomain equation. For $t \in (0, T]$ find v such that:

$$v = \mathcal{M}(v, \boldsymbol{d}, \boldsymbol{w}) \quad \text{in} \quad \hat{\Omega}_s. \tag{1}$$

  Then we define the gating variables and ionic concentrations condensed in a vector $\boldsymbol{w}$, modeled with the ODEs Ionic model equations. For $t \in (0, T]$ find $\boldsymbol{w}$ such that:

$$\boldsymbol{w} = \mathcal{I}(v, \boldsymbol{w}) \quad \text{in} \quad \hat{\Omega}_s. \tag{2}$$

- For the structure problem we define the structure displacement $\boldsymbol{d}$ modeled with the PDE Structure equation. For $t \in (0, T]$ find $\boldsymbol{d}$ such that:

$$\begin{cases} \boldsymbol{d} = \mathcal{S}(\boldsymbol{d}, \boldsymbol{w}) & \text{in } \hat{\Omega}_s, \quad (3a) \\ \dfrac{\partial \boldsymbol{d}}{\partial t} = \boldsymbol{u} & \text{on } \hat{\Sigma}, \quad (3b) \\ \sigma_s(\boldsymbol{d})\boldsymbol{n} = \sigma_f(\boldsymbol{u}, p)\boldsymbol{n} & \text{on } \Sigma, \quad (3c) \end{cases}$$

  where $\boldsymbol{u}$ is the fluid velocity, p is the fluid pressure, σ_f and σ_s are the fluid and structure Cauchy Stress tensors respectively. (3b) is the *kinematic condition* to ensure the continuity of velocity at the interface, and (3c) is the *dynamic condition* to ensure the continuity of forces at the interface, i.e. the Third Newton's Law. Moreover, the solution for the displacement $\boldsymbol{d}$ depends on $\boldsymbol{w}$ because the First Piola-Kirchhoff Stress Tensor of the Structure problem has also an active part depending on the Calcium concentration, i.e. one of the component of $\boldsymbol{w}$.

- For the fluid problem we define the fluid velocity $\boldsymbol{u}$ and the fluid pressure p modeled with the Navier Stokes Equation for incompressible fluids in Arbitrary Lagrangian Eulerian (ALE) Formulation. Moreover, we define the fluid displacement $\boldsymbol{d}_{ALE}$ necessary to compute the new fluid domain at each time step; this leads to the following geometric problem equipped with the *geometric condition* on the Fluid Structure interface Σ. For $t \in (0, T]$ find $\boldsymbol{d}_{ALE}$ such that:

$$\begin{cases} -\Delta \boldsymbol{d}_{ALE} = \boldsymbol{0} & \text{in } \hat{\Omega}_f, \quad (4a) \\ \boldsymbol{d}_{ALE} = \boldsymbol{d} & \text{on } \hat{\Sigma}. \quad (4b) \end{cases}$$

  Now we can compute the current fluid domain:
  $\Omega_f = \left\{ \boldsymbol{x} \in \mathbb{R}^3 : \boldsymbol{x} = \hat{\boldsymbol{x}} + \boldsymbol{d}_{ALE}, \hat{\boldsymbol{x}} \in \hat{\Omega}_f \right\}$,
  so that we can state the Navier Stokes equations in ALE formulation. For $t \in (0, T]$ find $(\boldsymbol{u}, p)$ such that:

$$\begin{cases} (\boldsymbol{u}, p) = \mathcal{F}(\boldsymbol{u}, \boldsymbol{d}_{ALE}, \boldsymbol{d}) & \text{in } \Omega_f \quad (5a) \\ \dfrac{\partial \boldsymbol{d}}{\partial t} = \boldsymbol{u} & \text{on } \Sigma, \quad (5b) \\ \sigma_s(\boldsymbol{d})\boldsymbol{n} = \sigma_f(\boldsymbol{u}, p)\boldsymbol{n} & \text{on } \Sigma, \quad (5c) \end{cases}$$

  where (5b) and (5c) are again the *kinematic* and *dynamic conditions*.

We can summarize the complete Electro Fluid Structure Interaction Problem.
Given $v_0, \boldsymbol{w}_0, \boldsymbol{d}_0, \boldsymbol{u}_0, p_0$ find for $t \in (0, T]$ $v, \boldsymbol{w}, \boldsymbol{d}, \boldsymbol{u}, p$ such that:

$$\begin{cases} v = \mathcal{M}(v, \boldsymbol{w}, \boldsymbol{d}) & \text{in} \quad \hat{\Omega}_s, \\ \boldsymbol{w} = \mathcal{I}(v, \boldsymbol{w}) & \text{in} \quad \hat{\Omega}_s, \\ -\Delta \boldsymbol{d_{ALE}} = \boldsymbol{0} & \text{in} \quad \hat{\Omega}_f, \\ \boldsymbol{d} = \mathcal{S}(\boldsymbol{d}, \boldsymbol{w}) & \text{in} \quad \hat{\Omega}_s, \\ (\boldsymbol{u}, p) = \mathcal{F}(\boldsymbol{u}, \boldsymbol{d}_{ALE}, \boldsymbol{d}) & \text{in} \quad \Omega_f, \\ \\ \boldsymbol{d_{ALE}} = \boldsymbol{d} & \text{on} \quad \hat{\Sigma}, \\ \boldsymbol{u} = \dfrac{\partial \boldsymbol{d}}{\partial t} & \text{on} \quad \Sigma, \\ \sigma_f(\boldsymbol{u}, p)\boldsymbol{n} = \sigma_s(\boldsymbol{d})\boldsymbol{n} & \text{on} \quad \Sigma. \end{cases} \tag{6}$$

3. Algorithms

To carry out the simulations we use three different schemes: *Scheme 1*, *Scheme 2* and our new Loosely-Coupled EFSI *Scheme 3*; they differ only on the treatment of the Fluid Structure Interaction problem. Indeed, *Scheme 1* solves the FSI Problem in a Monolithic fashion; on the other hand *Scheme 2* and *Scheme 3* make use of the partitioned Robin-Neumann Scheme, based on the splitting of the FSI problem in two problems:

(i) the fluid problem equipped with a Robin condition in place of the *kinematic condition* on the interface Σ:

$$\alpha_f \boldsymbol{u} + \sigma_f(\boldsymbol{u}, p)\boldsymbol{n} = \alpha_f \frac{\partial \boldsymbol{d}}{\partial t} + \sigma_s(\boldsymbol{d})\boldsymbol{n}; \tag{7}$$

(ii) the structure problem equipped with a Neumann condition, i.e. the *dynamic condition* (3c) on Σ.

The first common steps of the schemes are the following:

1. Solve the linearized ionic model equations to find $\boldsymbol{w}_{n+1}$:

$$\boldsymbol{w}_{n+1} = \mathcal{I}(v_n, \boldsymbol{w}_n) \quad in \quad \hat{\Omega}_s. \tag{8}$$

2. Solve the linearized monodomain equations to find v_{n+1}:

$$v_{n+1} = \mathcal{M}(v_n, \boldsymbol{d}_n, \boldsymbol{w}_{n+1}) \quad in \quad \hat{\Omega}_s. \tag{9}$$

3. Solve the geometric problem to find $\boldsymbol{d}_{ALE,n+1}$:

$$\begin{cases} -\Delta \boldsymbol{d}_{ALE,n+1} = \boldsymbol{0} & \text{in} \quad \hat{\Omega}_f, \\ \boldsymbol{d}_{ALE,n+1} = \boldsymbol{d}_n & \text{on} \quad \hat{\Sigma}. \end{cases} \tag{10}$$

4. Compute the current domain $\Omega_{f,n+1}$ and $\boldsymbol{u}_{ALE,n+1}$:

$$\Omega_{f,n+1} = \left\{ \boldsymbol{x} \in \mathbb{R}^3 : \boldsymbol{x} = \hat{\boldsymbol{x}} + \boldsymbol{d}_{ALE,n+1}(\hat{\boldsymbol{x}}), \hat{\boldsymbol{x}} \in \hat{\Omega}_f \right\},$$

$$\boldsymbol{u}_{ALE,n+1} = \frac{\boldsymbol{d}_{ALE,n+1} - \boldsymbol{d}_{ALE,n}}{\Delta t}.$$

Then the last step is done in the following ways, according to the considered scheme:

S1 5. Solve the non linear FSI problem in a Monolithic fashion to find $\boldsymbol{u}_{n+1}$, p_{n+1} and $\boldsymbol{d}_{n+1}$:

$$\begin{cases} \boldsymbol{d}_{n+1} = \mathcal{S}(\boldsymbol{d}_{n+1}, \boldsymbol{w}_{n+1}, \boldsymbol{d}_n) & \text{in} \quad \hat{\Omega}_s, \\ \boldsymbol{u}_{n+1} = \dfrac{\boldsymbol{d}_{n+1} - \boldsymbol{d}_n}{\Delta t} & \text{on} \quad \Sigma_{n+1}, \\ \sigma_f(\boldsymbol{u}_{n+1}, p_{n+1})\boldsymbol{n} = \sigma_s(\boldsymbol{d}_{n+1})\boldsymbol{n} & \text{on} \quad \Sigma_{n+1}, \\ (\boldsymbol{u}_{n+1}, p_{n+1}) = \\ \quad \mathcal{F}(\boldsymbol{u}_n, \boldsymbol{d}_{ALE,n+1}, \boldsymbol{d}_n; \Omega_{f,n+1}) & \text{in} \quad \Omega_{f,n+1}. \end{cases} \tag{11}$$

S2 5. Solve in a loop until convergence the FSI problem using the implicit Robin-Neumann algorithm, defining the apex $^{(k)}$, that indicates the k-th iteration of the loop.
For ($k > 0$ && **Stopping criterion**) **do**:

-5a. solve the linearized fluid problem equipped with a Robin condition on the interface:

$$\begin{cases} (\boldsymbol{u}_{n+1}^{(k)}, p_{n+1}^{(k)}) = \\ \quad = \mathcal{F}(\boldsymbol{u}_n, \boldsymbol{d}_{ALE,n+1}, \boldsymbol{d}_n; \Omega_{f,n+1}) & \text{in } \Omega_{f,n+1}, \\ \\ \alpha_f \boldsymbol{u}_{n+1}^{(k)} + \sigma_f(\boldsymbol{u}_{n+1}^{(k)}, p_{n+1}^{(k)})\boldsymbol{n} = \\ \quad = \alpha_f \dfrac{\boldsymbol{d}_{n+1}^{(k-1)} - \boldsymbol{d}_n}{\Delta t} + \sigma_s(\boldsymbol{d}_{n+1}^{(k-1)})\boldsymbol{n} & \text{on } \Sigma_{n+1}. \end{cases} \tag{12}$$

-5b. solve the non linear Structure problem equipped with a Neumann condition on the interface:

$$\begin{cases} \boldsymbol{d}_{n+1}^{(k)} = \mathcal{S}(\boldsymbol{d}_{n+1}^{(k)}, \boldsymbol{w}_{n+1}, \boldsymbol{d}_n) & \text{in} \quad \hat{\Omega}_s, \\ \sigma_s(\boldsymbol{d}_{n+1}^{(k)})\boldsymbol{n} = \sigma_f(\boldsymbol{u}_{n+1}^{(k)}, p_{n+1}^{(k)})\boldsymbol{n} & \text{on} \quad \Sigma_{n+1}. \end{cases} \tag{13}$$

S3 5. solve the linearized Fluid Problem equipped with a Robin condition on the interface:

$$\begin{cases} (\boldsymbol{u}_{n+1}, p_{n+1}) = \\ \quad = \mathcal{F}(\boldsymbol{u}_n, \boldsymbol{d}_{ALE,n+1}, \boldsymbol{d}_n; \Omega_{f,n+1}) & \text{in } \Omega_{f,n+1}, \\ \alpha_f \boldsymbol{u}_{n+1} + \sigma_f(\boldsymbol{u}_{n+1}, p_{n+1})\boldsymbol{n} = \\ \quad = \alpha_f \dfrac{\boldsymbol{d}_n - \boldsymbol{d}_{n-1}}{\Delta t} + \sigma_s(\boldsymbol{d}_n)\boldsymbol{n} & \text{on } \Sigma_{n+1}; \end{cases} \tag{14}$$

6. solve the non-linear Structure Problem equipped with a Neumann condition on the interface:

$$\begin{cases} \boldsymbol{d}_{n+1} = \mathcal{S}(\boldsymbol{d}_{n+1}, \boldsymbol{w}_{n+1}, \boldsymbol{d}_n) & \text{in} \quad \hat{\Omega}_s, \\ \sigma_s(\boldsymbol{d}_{n+1})\boldsymbol{n} = \sigma_f(\boldsymbol{u}_{n+1}, p_{n+1})\boldsymbol{n} & \text{on} \quad \Sigma_{n+1}. \end{cases} \tag{15}$$

4. Choice of simulation parameters

To assess the physiological behavior of the numerical results of our simulations we have defined physiological indicators that have to satisfy precise requirements. Therefore, we have calibrated the simulation parameters using *Scheme 1* and trying to reproduce a behavior closer as possible to the physiological one. For what concerns the choice of the Robin interface parameter α_f (see (7)) we have carried on a theoretical analysis on a simplified problem; this analysis gave us a range that is not expected to be optimal for our EFSI Problem due to the strong simplification of the simplified theoretical problem. However, it is important to have an initial guess sufficiently close to the effective range. In this sense the theoretical analysis is useful. The theoretical optimal range for the simplified problem was computed by professor Giacomo Gigante:

$$\alpha_f \in [1906.4, 2415.1][\frac{kg}{m^2 \cdot s}]. \tag{16}$$

5. Numerical Results

In what follows, the unit $[\frac{kg}{m^2 \cdot s}]$ for the parameter α_f will be understood. This abuse of notation is done for the sake of simplicity in notation, tables and figures. We will call the results obtained using *Scheme j*: *G-j*. We have simulated our EFSI Problem using our new *Loosely-coupled EFSI Scheme 3* with different values of α_f, comparing the results with the one obtained using *Scheme 1*. In figure 2 and figure 3 we have reported a comparison of the results obtained using *Scheme 1* and *Scheme 3* with different values of α_f in terms of the time evolution of the ventricular chamber volume and pressure. Moreover in figure 4 and 5 some numerical results are shown.

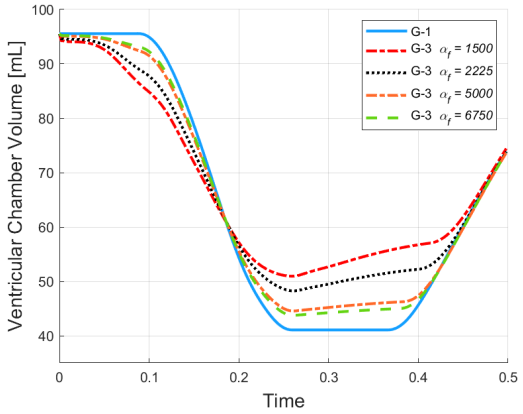

Figure 2: Comparison of the time evolution of the ventricular chamber volume obtained using *Scheme 1* and *Scheme 3* with different values of α_f.

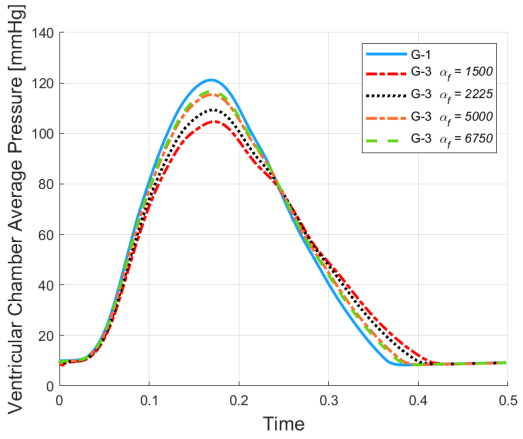

Figure 3: Comparison of the time evolution of the ventricular chamber average pressure obtained using *Scheme 1* and *Scheme 3* with different values of α_f.

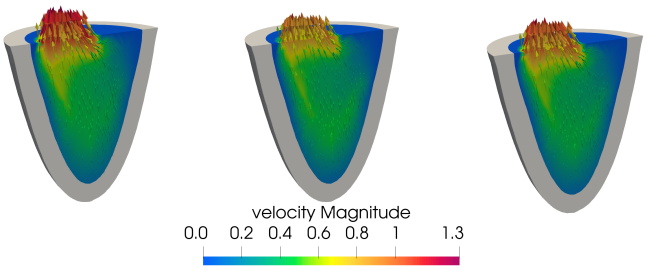

(a) *G-1*. (b) *G-3* $\alpha_f = 2225$ (c) *G-3* $\alpha_f = 5000$.

Figure 4: Comparison of the numerical solutions for the blood velocity magnitude obtained with *G-1* and *G-3* with different values of α_f. A time instant during the ejection phase is shown: $t = 0.17s$.

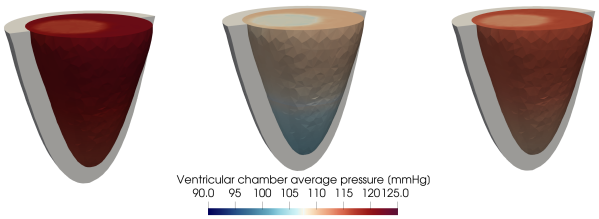

(a) *G-1*. (b) *G-3* $\alpha_f = 2225$. (c) *G-3* $\alpha_f = 5000$.

Figure 5: Comparison of the numerical solutions for the ventricular average chamber pressure obtained with *G-1* and *G-3* with different values of $alpha_f$. The time instant at which the maximum pressure p_{max} is reached is shown, i.e. $t = 0.17s$.

We can observe from figure 2 that using *Scheme 3* we have an inaccuracy in reproducing the isovolumic phases; this issue influences the time evolution of pressure and velocity, leading to lower values of average maximum pressure and velocity as one can observe in figure 3 and 5. However using *Scheme 3* we have obtained stable and physiologically reasonable results $\forall \alpha_f$ such that $1500 \leq \alpha_f \leq 6750$, but we suggest to use the range $1500 \leq \alpha_f \leq 5000$ due to the fact that the values $5000 < \alpha_f \leq 6750$ turns out to be a zone of transition towards non converging simulations. Notice that the theoretical range (16) is completely included in the just defined one; indeed, using values picked from the theoretical range we obtained stability and a certain level of accuracy in reproducing physiological results (error $\sim 10\%$). Anyway if we want to obtain more accurate results, we need to perform a manual calibration of the Robin interface parameter, e.g. with $\alpha_f = 5000$ we obtain an error of $\sim 4\%$ in reproducing physiological results.
For what regards the computational cost, we have experienced that *Scheme 3* using the calibrated optimal parameter (i.e. $\alpha_f = 5000$) is $\sim 35\%$ faster than *Scheme 1*, as one can see from table 1, where a comparison between *Scheme 1,2* and *3* is done in terms of computational cost and accuracy in reproducing the isovolumic phases (we report an indicator ILI: Isovolumic Loss Indicator that quantifies the percentage amount of volume loss/gain during the isovolumic phases), that is the most reliable indicator to discriminate the accuracy of the obtained results; indeed, the isovolumic phases influence all the other physiological indicators.

	G-1	*G-2*(22250)	*G-3*(5000)
CPU_{Time} $[s]$	7070	30000	4724
ILI $[s]$	0.01%	0.01%	$< 4\%$

Table 1: Comparison of the computational costs and Isovolumic Volume Indicators obtained in *G-1* and in *G-2*, *G-3* with the optimal calibrated parameters. We have simulated $0.5s$ with $\Delta t = 2 \cdot 10^{-4}$.

Moreover, we have also investigated *Scheme 2* with different choices for α_f. We have experienced that it gives at convergence the same iden-

tical results of *Scheme 1* for a wide range of parameters. However, *Scheme 2* is computationally inefficient; indeed, even with the calibrated empirical optimal Robin interface parameter α_f is four times slower than *Scheme 1*.
Finally, we have explored two possibilities to reduce the issue of *Scheme 3* in capturing the isovolumic phases: use *Scheme 3* halving the time step or perform 2 iterations instead of 1 in the FSI Robin-Neumann loop. These two choices lead to better results in reproducing the physiological behavior but also to an increase in computational costs.

6. Conclusions

We have obtained encouraging results with our proposed new Loosely-coupled Scheme for cardiac EFSI Problem. The range of theoretical values of α_f for the Robin interface parameter gave stability and accuracy with an error of $\sim 10\%$ in reproducing a physiological behavior. However, to obtain a higher level of accuracy a manual calibration of the Robin parameter α_f is needed; with the calibrated empirical optimal Robin interface parameter α_f we obtained an error of $\sim 3/4\%$ in reproducing a physiological behavior. We have established an empirical range for the choice of the Robin parameters to obtain stable, accurate and computationally efficient simulations; we have ascertained that the theoretical range is completely contained inside it. Comparing this new *Loosely-coupled EFSI Scheme 3* with the *Staggered E-Monolithic FSI Scheme 1*, we have noticed that:

- *Scheme 1* perfectly captures the isovolumic phases, while with *Scheme 3* we commit an error in reproducing such phases due to the spurious numerical fluxes given by the explicit treatment of the FSI coupling conditions. However, with the optimal empirical value α_f this error is less than 4%, whilst using values in the theoretical range (16) we commit an error of $\sim 8\%$.
- *Scheme 3* is $\sim 35\%$ faster than *Scheme 1* and has also the advantage of being modular, i.e. we can use different already existing solvers.

References

[1] M. Bucelli, L. Dedè, A. Quarteroni, and C. Vergara. Partitioned and monolithic algorithms for the numerical solution of cardiac fluid-structure interaction. *MOX report n. 78/2021*, 2021.

[2] G. Gigante and C. Vergara. On the choice of interface parameters in Robin–Robin loosely coupled schemes for fluid–structure interaction. *Fluids*, page 109–119, 2021.

[3] G. Gigante and C. Vergara. On the stability of a loosely-coupled scheme based on a Robin interface condition for fluid-structure interaction. *Computers and Mathematics with Applications*, page 109–119, 2021.

[4] F. Regazzoni, M. Salvador, P. C. Africa, M. Fedele, L. Dedè, and A. Quarteroni. A cardiac electromechanics model coupled with a lumped parameters model for closed-loop blood circulation. *Journal of Computational Physics*, 2022.